

Composite Material Robot Manipulator with Joint Flexibility- Mode and Mode Shape Simulation



Ramalingam S, Rasool Mohideen S, Sridhar P S

Abstract: Simulation of composite material robot manipulator with joint flexibility is initiated. The lightweight three types of composite material manipulator links with different joint stiffness are considered for vibration mode and mode shape simulation. The model and its motion equations are obtained by using assumed mode method incorporating and joint flexibility. The structural flexibility of a composite material also included in the analyses. The purpose of simulation to predict the behavior of composite material links, which is inevitable for replacement of bulky manipulators. To reach a set point of flexible link manipulator in a work volume with vibration accuracy is analyzed. The thin flexible link for precise positioning will face transient vibration problems. The flexible deflection and residual vibration are affect the positioning of end point. The source of vibration of a manipulator is due to light structural weight when it is rotated by the actuator. The lightweight link will move faster, but the unwanted vibration in the link is raised. To reduce this vibration issue, without compromising the light weight material, the simulation is carried out.

Keywords: Composite material, Kevlar epoxy, Graphite epoxy, Aluminium, mode of vibration.

I. INTRODUCTION

The composite material flexible links are inevitable in field of robotics; it has many application and prime solution to replace rigid manipulators. The existing manipulators consume more power, response time lack, heavy mass and difficult to maneuver. The advanced lightweight material manipulators take less power, quick response time, safe operations and reduced payload to weight ratio [1]. In the hostile environment also the flexible link robot manipulators are now commonly employed, such as atomic plant for handling radioactive materials [2]. However, in flexible manipulators system some difficulties arise which are residual vibration and position accuracy.

The distributed flexibility and behavior of the system, the dynamics are very complex. The issue is arrived to precise positioning requirement, vibration due to system flexibility [3-4]. By selecting suitable material for manipulator and adding appropriate control techniques the effect of shivering amplitude of vibration and system settling time can be reduced.

The inclusion of flexible materials has some advantages in the fields such as space shuttle, solar panel [5] and underwater as well as high speed energy efficient manipulation. The material like, aluminum, Kevlar epoxy composite and Graphite epoxy composite for single link flexible manipulators have taken for vibration analysis. Assumed mode method is used in this research to analyze the oscillatory behavior of manipulator for three category materials and finally concluded the best suited material for single link flexible manipulator.

II. MATERIALS AND METHODS

A. MATERIALS

The hybrid composite is some sort of fibre-reinforced plastic (FRP) materials, in which a combination of two different fibres with epoxy resin is integrated into a single matrix. In any combination of dissimilar fibre materials with epoxy resin is treated as a hybrid. The example for structural composite material is rigid plastic foam bonded with thin skins of some high-performance FRPs. A mixing of fibrous and particulate fillers in a single resin or metal matrix produces another kind of hybrid composite.

In recent scenario, the cost of material is significant by comparison with the other and the advantages of optimizing properties. In an aerospace application, purpose of using hybrids is to utilize the natural toughness of graphite fibre-reinforced plastics (GRP) or Kevlar-fibre-reinforced plastics (KFRP) to avoid brittleness of typical CFRP. The important aspect of using hybrids is to provide adequate material stiffening, strengthening and toughening of the material which has a plenty of advantages. The three types of materials are extracted from literature and used for simulation and numerical analysis is conducted. By comparative study the best suited material among three is notified.

B. METHODS

The schematic diagram shows that the model of single link with parameters is marked in the figure 1. The motor is fixed and their shaft is connected to the hub. The hub inertia is I_h . The control input torque (τ) is applied to the motor. The hub and manipulator as a single link rotate in a horizontal plane. The co-ordinate frames X_0-O-Y_0 and X_1-O-Y_1 are attached to the rigid body frame.

Manuscript published on November 30, 2019.

* Correspondence Author

Ramalingam S*, Department of Mechanical Engineering, B S A Crescent Institute of Science and Technology, Chennai India. Email: sengalaniramalingam@gmail.com

Dr. Rasool Mohideen S, Professor and Dean, School of Mechanical Science, B S A Crescent Institute of Science and Technology, Chennai India. Email: dean.sms@crescent.education

Prof. Sridhar P S, Professor, Department of Marine Engineering, AMET University, Chennai India. Email: monathatha@gmail.com

© The Authors. Published by Blue Eyes Intelligence Engineering and Sciences Publication (BEIESP). This is an [open access](http://creativecommons.org/licenses/by-nc-nd/4.0/) article under the CC-BY-NC-ND license <http://creativecommons.org/licenses/by-nc-nd/4.0/>

Due smaller angular rotation $\theta(t)$ of pinned free manipulator, the flexible deflection $u(x, t)$ and total displacement of a link is calculated as $y(x, t) = u(x, t) + x\theta(t)$.

For equation of motion, the energy associated to the systems is calculated. The kinetic (KE) and potential (PE) energies of the system with end payload are included in equation.

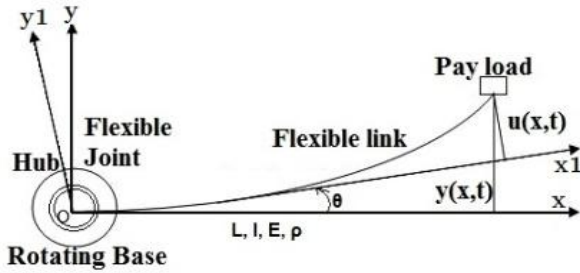


Figure.1 Schematic diagram of flexible link

In the equation of motion, a non-conservative work for a given input torque to the system is calculated. Using Hamilton [6], and lagrangian techniques, by ignoring the rotary inertia and shear deformation effects, the first two modes are used for modeling, after a mathematical manipulation, the link equation become with four boundary conditions. The flexible deflection $u(x, t)$ is determined and substituted in the equation which yields the equation of motion in terms total deflection of $y(x, t)$.

III. DYNAMIC EQUATION

By using the boundary conditions, a fourth order partial differential equation is obtained. This equation describes the motion of flexible link manipulator. The solution is obtained by using assumed mode method [7], and lagrangian approach. The flexible deflection is the product, spatial and time function. The flexible deflection $u(x, t)$ is approximated by [8],

$$u(x, t) = \sum_{i=1}^n \phi_i(x)q_i(t) + \phi_2(x)q_2(t) + \dots + \phi_i(x)q_i(t), \text{ for } i=1,2,3,\dots,n \quad \text{--- (1)}$$

The input torque $(T)_{in}$ is set to zero. The orthogonality relationship of the second derivatives, which is true for a system with only structural flexibility, hence the total flexible deflection from the initial co-ordinate is determined by

$$y(x, t) = \sum_{i=1}^n \phi_i(x)q_i(t) + \phi_2(x)q_2(t) + \dots + \phi_i(x)q_i(t), \text{ for } i=1,2,3,\dots,n \quad \text{--- (2)}$$

The spatial function $\phi_i(x)$ is the mode shape, which is purely function of displacement and $q_i(t)$ time function. To substitute the value of $y(x, t)$ in equation, this yields ordinary differential equation of fourth order and second order equation. The solution for fourth order equation is

$$\phi_i(x) = A_i \sin \beta_i x + B_i \sinh \beta_i x + C_i \cos \beta_i x + D_i \cosh \beta_i x \quad \text{--- (3)}$$

Where, $i = 1, 2, 3, \dots, n$ and A_i, B_i, C_i and D_i are mode shape constants. To simplify the computation the following parameters are used for equation,

$$\beta^4 = \left(\frac{\rho}{EI} \right) \omega^2, \lambda = \beta L$$

$$I_b = \frac{\rho L^3}{3}, \epsilon = \frac{I_h}{3I_b} \quad \text{--- (4)}$$

$$\eta = \frac{M_p L^2}{3I_b}, K_c = \frac{K_t}{EI/L}$$

From the above, the characteristic equations of the system are derived and the equation is solved for its Eigen values [9],

$$D(\lambda) = (-\epsilon \lambda^4 + K_c) [1 + \cos \lambda \cosh \lambda + \eta \lambda (\cos \lambda \sinh \lambda - \sin \lambda \cosh \lambda)] - \lambda (\sin \lambda \cosh \lambda - \cos \lambda \sinh \lambda + 2\eta \lambda \sin \lambda \sinh \lambda) = 0 \quad \text{--- (5)}$$

To find the frequencies and mode shapes of the system, the values of λ_i are obtained from the characteristic equation and the corresponding values of constants A_i, B_i, C_i and D_i are also calculated. Assume that the value of $D_i = 1$ (one) according to assumed mode method. The normalization relations, the expression for kinetic and potential energy are determined.

IV. STATE SPACE FORM

For controlling a flexible link of robot manipulator, the Lagrangian formulation is represented in a state space form to control [10] and [11],

$$\dot{X} = AX + Bu \quad \text{--- (6)}$$

$$A = \begin{bmatrix} 0 & 1 & 0 & 0 & 0 & 0 & \dots & 0 & 0 \\ 0 & 0 & 0 & 0 & 0 & 0 & \dots & 0 & 0 \\ 0 & 0 & 0 & 1 & 0 & 0 & \dots & 0 & 0 \\ 0 & 0 & -\omega_1^2 & -2\xi_1 \omega_1 & 0 & 0 & \dots & 0 & 0 \\ 0 & 0 & 0 & 0 & 0 & 1 & \dots & 0 & 0 \\ 0 & 0 & 0 & 0 & -\omega_2^2 & -2\xi_2 \omega_2 & \dots & 0 & 0 \\ \dots & \dots \\ 0 & 0 & 0 & 0 & 0 & 0 & \dots & 0 & 1 \\ 0 & 0 & 0 & 0 & 0 & 0 & \dots & \omega_n^2 & -2\xi_n \omega_n \end{bmatrix} \quad \text{--- (7)}$$

$$X^T = [q_0 \quad \dot{q}_0 \quad q_1 \quad \dot{q}_1 \quad \dots \quad q_n \quad \dot{q}_n] \quad \text{--- (8)}$$

$$B^T = \frac{1}{I_T} \left[0 \quad 1 \quad 0 \quad \frac{d\phi_1(0)}{dx} \quad \dots \quad 0 \quad \frac{d\phi_n(0)}{dx} \right] \quad \text{--- (9)}$$

$$B^T = \frac{1}{I_T} \left[0 \quad 1 \quad 0 \quad \frac{d\phi_1(0)}{dx} \quad \dots \quad 0 \quad \frac{d\phi_n(0)}{dx} \right] \quad \text{--- (10)}$$

$$C = \begin{bmatrix} 1 & 0 & \frac{d\phi_1^2(1)}{dx^2} & 0 & \dots & \frac{d\phi_n^2(1)}{dx^2} & 0 \\ 1 & 0 & \frac{d\phi_1(0)}{dx} & 0 & \dots & \frac{d\phi_n(0)}{dx} & 0 \\ 0 & 1 & 0 & \frac{d\phi_1(0)}{dx} & \dots & 0 & \frac{d\phi_n(0)}{dx} \end{bmatrix} \quad \dots (11)$$

$$D = (0) \quad \dots (12)$$

The output is $y = Cx + D$ --- (13)

Table. I Parameters of Aluminium (960mmx19.01mmx3.2mm) [12]

| Aluminium Material | Young's Modulus (E) (N/m ²) | Density (ρ) kg/m ³ | Cross Sectional area (a) (m ²) | Mass of link (m) (kg) | Moment of inertia (I) (m ⁴) | Rigidity (EI) (Nm ²) | Beam inertia (I _b) (kg m ²) | Hub Inertia (I _h) (kg m ²) |
|--------------------|---|-------------------------------|--|-----------------------|---|----------------------------------|---|--|
| | 71e9 | 2710 | 6.083e-5 | 0.158 | 5.192e-11 | 3.687 | 0.049 | 5.86e-4 |

Table. II Properties of Graphite/Epoxy [13]

| Graphite/Epoxy Composite | Size of Link in (mm) | Sectional area (a) (m ²) | Density of Material (kg/m ³) | Moment of inertia (I) (m ⁴) | Young's Modulus E _x (N/m ²) | Young's Modulus E _y (N/m ²) |
|--------------------------|----------------------|--------------------------------------|--|---|--|--|
| | 960x19.01x3.2 | 6.083e-5 | 1600 | 5.192e-11 | 181e9 | 10.3e9 |

Table. III Properties of Kevlar-49/Epoxy [13]

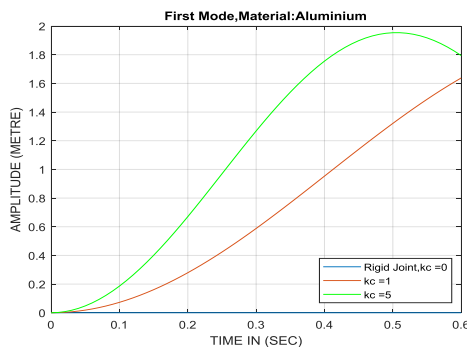
| Kevlar/Epoxy Composite | Size of Link in (mm) | Sectional area (a) (m ²) | Density of material kg/m ³ | Moment of inertia(I) (m ⁴) | Young's Modulus E _x (N/m ²) | Young's Modulus E _y (N/m ²) |
|------------------------|----------------------|--------------------------------------|---------------------------------------|--|--|--|
| | 960x19.01x3.2 | 6.083e-5 | 1360 | 5.192e-11 | 76e9 | 5.5e9 |

V. RESULTS AND DISCUSSION

Based on the expression, the above material like, aluminium and hybrid composite material has taken for numerical study, a complete MATLAB algorithm has been written for simulation study [14]. For first case the link manipulator is made of aluminium, with uniform rectangular cross section of size 19.01mmx3.2mm and length is 960mm. The modulus of the material is, 71e9 N/m². The mass density of the material is assumed to be ρ = 2710 kg/m³, mass moment of inertia is, I = 5.192e-11 m⁴, I_T = 0.8 kgm² and viscous damping co-efficient is, ζ = 0.015. Using the above data frequency and damped natural frequency are calculated.

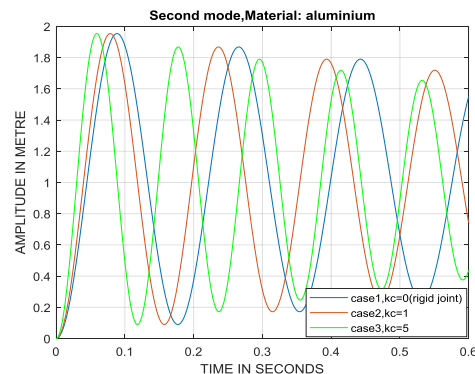
A comparison among different joint flexibility is made in order to demonstrate the importance of incorporating joint flexibility into the dynamic model (case-1 K_c = 0, case-2 K_c = 1, case-3 K_c = 5). The response of unit step input torque for the open loop system was calculated and simulation results are shown in fig (2).

A. ALUMINIUM MAMODE PLOTS



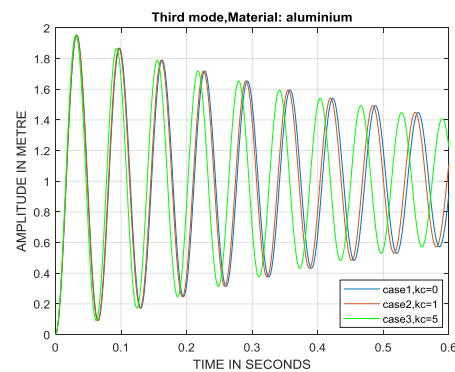
Case 1: k_c = 0, λ₀ = 0, Case 2: k_c = 1, λ₁ = 0.8657
Case.3: k_c = 5, λ₁ = 1.1009.

Figure. 2 First mode-3 types of Joint flexibility.



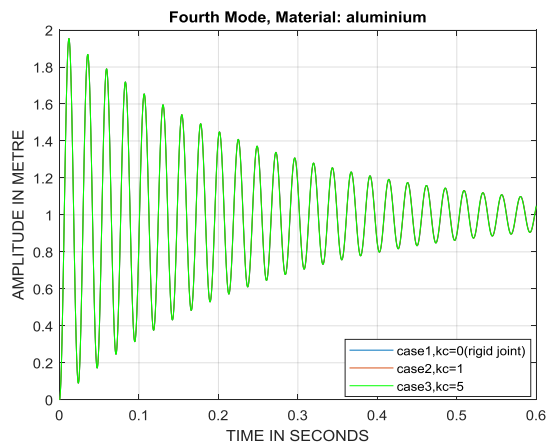
Case 1: k_c = 0, λ₁ = 2.630312, Case 2: k_c = 1, λ₂ = 2.7899,
Case.3: k_c = 5, λ₂ = 3.2175

Figure. 3 Second mode-3 types of Joint flexibility.



Case 1: k_c = 0, λ₂ = 4.3385, Case 2: k_c = 1, λ₃ = 4.3562,
Case.3: k_c = 5, λ₃ = 4.4409

Figure. 4 Third mode -3 types of Joint flexibility.



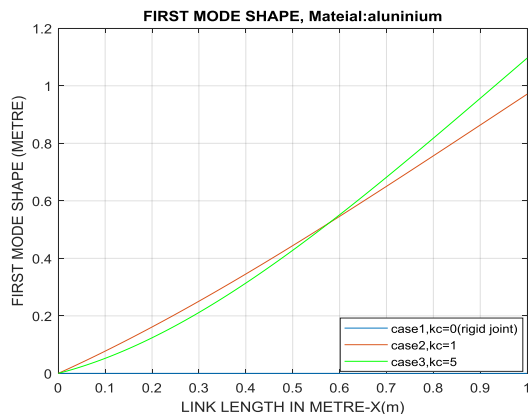
Case 1: $k_c = 0, \lambda_3 = 7.1904$, Case 2: $k_c = 1, \lambda_4 = 7.19083$
Case 3: $k_c = 5, \lambda_4 = 7.1927$

Figure 5 Fourth mode -3 types of Joint flexibility.

The maximum vibration amplitude for first mode of three cases i.e., case-1 (stiffness co-efficient $k_c = 0$, but flexible system not equal to zero), case-2 (stiffness co-efficient $k_c = 1$) is 1.6377m, case-3 (stiffness co-efficient $k_c = 5$) is 1.9536m. The maximum vibration amplitude for second mode case1, i.e. rigid mode stiffness co-efficient ($k_c = 0$) is 1.9538m, case-2 (stiffness co-efficient $k_c = 1$) is 1.9539m, case-3 (stiffness co-efficient $k_c = 5$) is 1.9538m. For third mode the maximum vibration amplitude for case-1 ($k_c = 0$), case-2 ($k_c = 1$), and case-3 ($k_c = 5$) are 1.9540m, 1.9540m and 1.9540m respectively. From the fourth mode maximum amplitude vibration for case1 ($k_c = 0$), case-2 ($k_c = 1$), case-3 ($k_c = 5$), are 1.9396, 1.9385 and 1.9345m respectively. The values for third and fourth mode amplitudes are very low and amplitudes are reducing slowly as shown in fig (4) and fig (5). The first two modes are used to control the manipulator system.

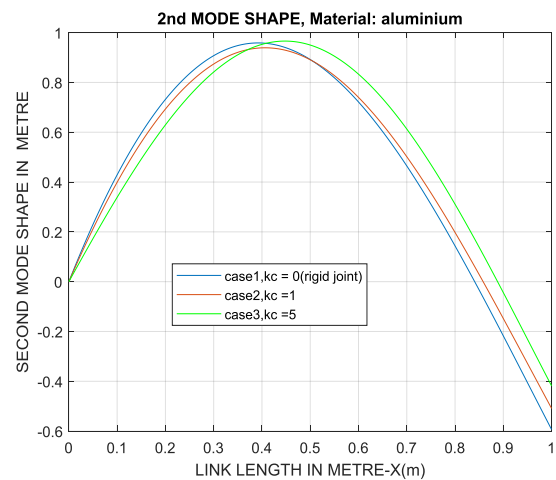
B. ALUMINIUM: MODE SHAPES [15]

Fig (6) and fig (7) gives the first mode shape for two flexible links and second mode shape for three flexible links at different position along the single link manipulator and up to $x = 1m$. The node point for first mode is at 0.570m. The second mode shape have been plotted and found that the node is shifted to 0.5m for case-1 and case-2. For case-2 and case-3 node is shifted to left hand side of the link with stiffness co-efficient is higher.



Case 1: $k_c = 0, \lambda_0 = 0$, Case 2: $k_c = 1, \lambda_1 = 0.965716$,
Case.3: $k_c = 5, \lambda_1 = 1.100850$.

Figure 6: First mode shape for three cases.



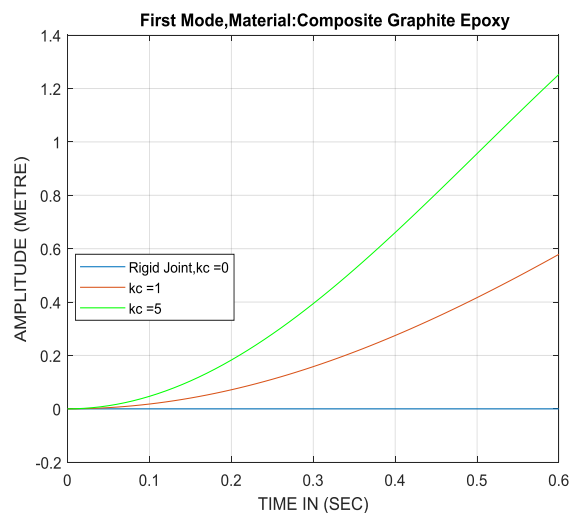
Case 1: $k_c = 0, \lambda_1 = 2.630312$, Case 2: $k_c = 1, \lambda_2 = 2.789944$,
Case.3: $k_c = 5, \lambda_2 = 3.217521$.

Figure 7: Second mode shape for three cases.

C. GRAPHITE/EPOXY PARAMETER

The second material, hybrid composite graphite epoxy, is simulated through MATLAB program. The graphite epoxy is the robotic link manipulator with uniform sectional area as it is in the case-1. The elastic modulus is $10.3e9 N/m^2$. The mass density of the material is $\rho = 1600 kg/m^3$, mass moment of inertia (I), viscous damping co-efficient (ζ) are same as in the case-1. Using the above data frequency and damped natural frequency are calculated.

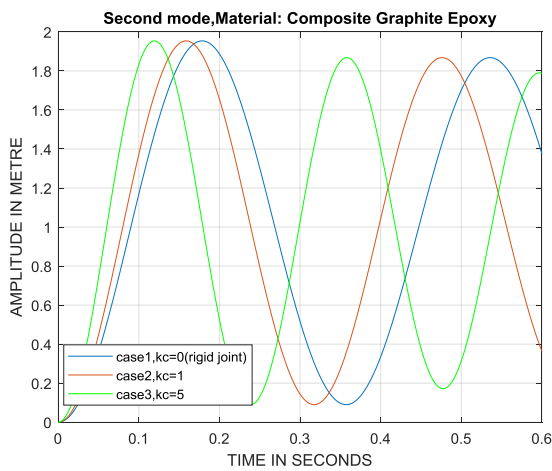
GRAPHITE/EPOXY MODE PLOTS



Case 1: $k_c = 0, \lambda_0 = 0$, Case 2: $k_c = 1, \lambda_1 = 0.8657$
Case.3: $k_c = 5, \lambda_1 = 1.1009$.

Figure 8 First mode-3 types of Joint flexibility.

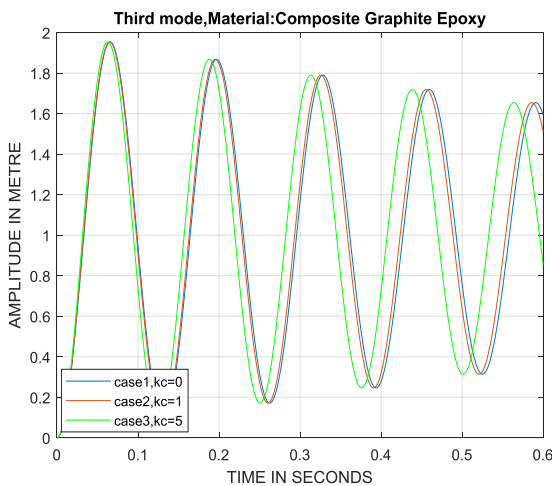
The vibration amplitude for first mode of three cases i.e., case-1 (stiffness co-efficient $k_c = 0$) is not equal to zero. Case-2 (stiffness co-efficient $k_c = 1$) is 0.4980m, case-3 (stiffness co-efficient $k_c = 5$) is 1.230m.



Case 1: $k_c = 0$, $\lambda_1 = 2.630312$, Case 2: $k_c = 1$, $\lambda_2 = 2.7899$, Case 3: $k_c = 5$, $\lambda_2 = 3.2175$

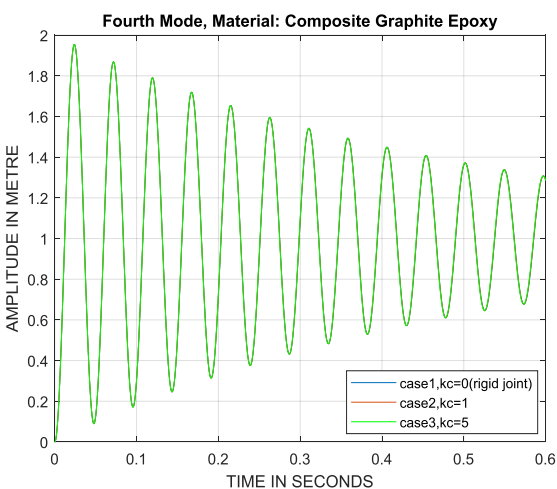
Figure. 9 Second mode-3 types of Joint flexibility.

The second mode amplitude of case 1, i.e. rigid mode stiffness co-efficient ($k_c = 0$) is 1.980m, case-2 (stiffness co-efficient $k_c = 1$) is 1.980m, case-3 (stiffness co-efficient $k_c = 5$) is 1.980m.



Case 1: $k_c = 0$, $\lambda_2 = 4.3385$, Case 2: $k_c = 1$, $\lambda_3 = 4.3562$, Case 3: $k_c = 5$, $\lambda_3 = 4.4409$

Figure. 10 Third mode -3 types of Joint flexibility



Case 1: $k_c = 0$, $\lambda_3 = 7.1904$, Case 2: $k_c = 1$, $\lambda_4 = 7.1908$, Case 3: $k_c = 5$, $\lambda_4 = 7.1927$

Figure. 11 Fourth mode -3 types of Joint flexibility.

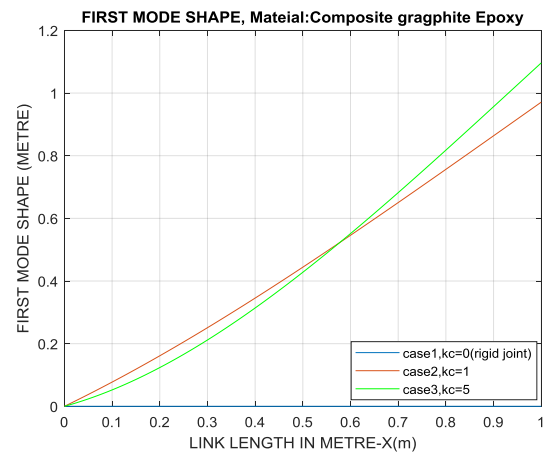
For third mode amplitude for case-1 ($k_c = 0$), case-2 ($k_c = 1$), and case-3 ($k_c = 5$) are 1.9540m, 1.9540m and 1.9540m respectively. But the amplitude is decaying.

From the fourth mode maximum amplitude vibration for case1 ($k_c = 0$), case-2 ($k_c = 1$), case-3 ($k_c = 5$), in all three cases 1.9540m respectively. The values of amplitudes in all four modes were reduced as shown in fig (8) to fig (11). Fourth mode amplitude was low at 0.6sec.

D. GRAPHITE /EPOXY MODE SHAPE 1, 2

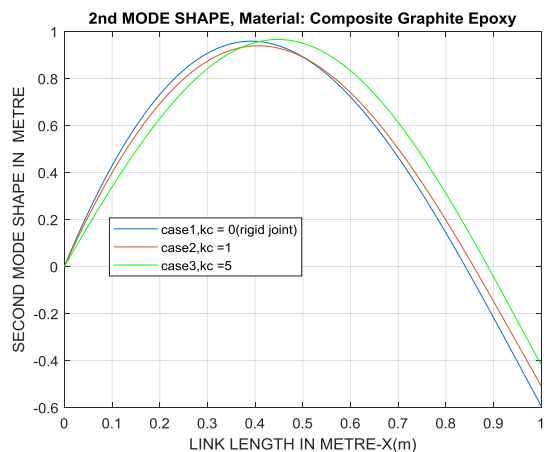
Fig (12) and fig (13) gives the first mode shape for flexible links and second mode shape for three flexible links at different position along the manipulator up to $x = 1$ m.

The node point for first mode is at 0.570m. In the second mode shape found that the node is shifted to 0.5m for case-1 and case-2 and case-2 and case-3 node is shifted towards left with higher stiffness.



Case 1: $k_c = 0$, $\lambda_0 = 0$, Case 2: $k_c = 1$, $\lambda_1 = 0.965716$, Case 3: $k_c = 5$, $\lambda_1 = 1.100850$.

Figure 12 First mode shapes for three cases.



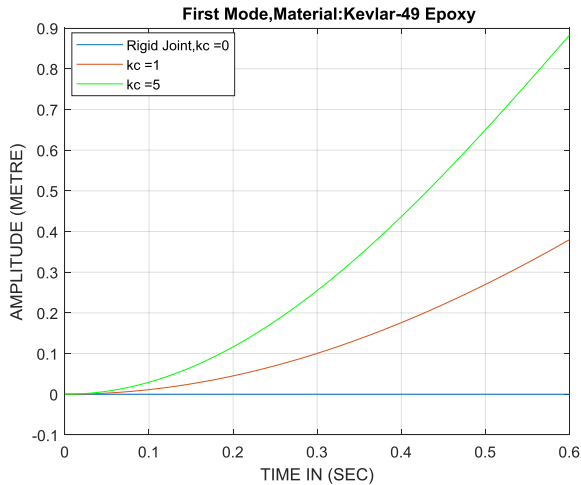
Case 1: $k_c = 0$, $\lambda_1 = 2.630312$, Case 2: $k_c = 1$, $\lambda_2 = 2.789944$, Case 3: $k_c = 5$, $\lambda_2 = 3.217521$.

Figure 13 Second mode shapes for three cases.

E. KEVLAR-49 EPOXY MODE PLOTS

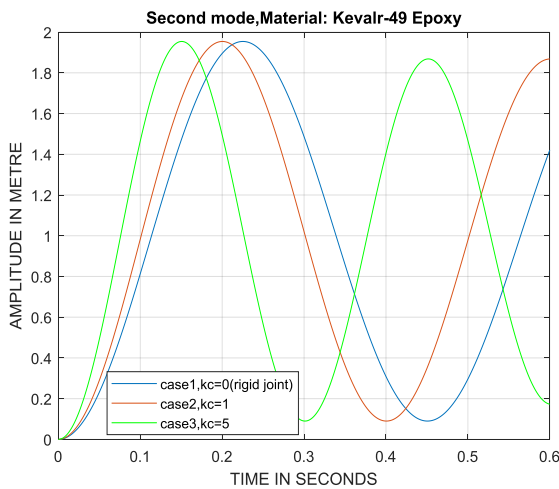
The same size of the link is considered for third material. The modulus of the kevlar-49 material is $5.5e9$ N/m². The density of the material is $\rho = 1360$ kg/m³ and other parameters are same as first material. The output response for different joint flexibility effect of three cases,

(case-1 $K_c = 0$, case-2 $K_c = 1$, case-3 $K_c = 5$) as shown in fig (14) to fig (17).



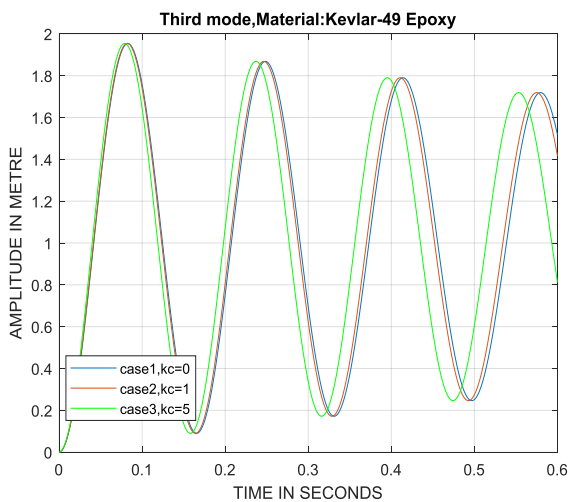
Case 1: $k_c = 0$, $\lambda_0 = 0$, Case 2: $k_c = 1$, $\lambda_1 = 0.8657$
Case.3: $k_c = 5$, $\lambda_1 = 1.1009$.

Figure. 14 First mode-3 types of Joint flexibility.



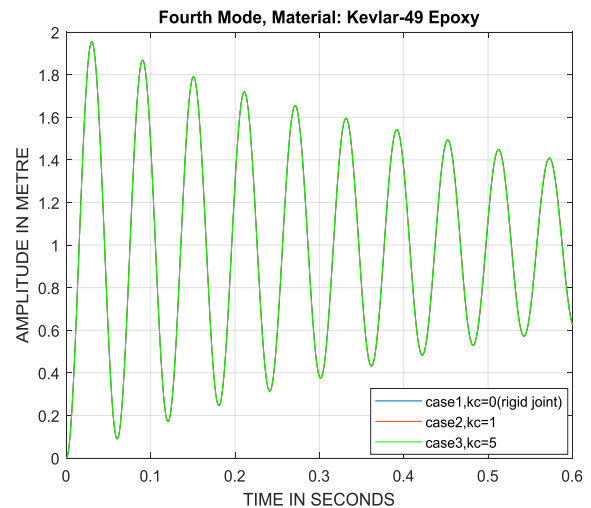
Case 1: $k_c = 0$, $\lambda_1 = 2.630312$, Case 2: $k_c = 1$, $\lambda_2 = 2.7899$,
Case.3: $k_c = 5$, $\lambda_2 = 3.2175$

Figure. 15 Second mode-3 types of Joint flexibility.



Case 1: $k_c = 0$, $\lambda_2 = 4.3385$, Case 2: $k_c = 1$, $\lambda_3 = 4.3562$,
Case.3: $k_c = 5$, $\lambda_3 = 4.4409$

Figure. 16 Third mode -3 types of Joint flexibility



Case 1: $k_c = 0$, $\lambda_3 = 7.1904$, Case 2: $k_c = 1$, $\lambda_4 = 7.1908$
Case 3: $k_c = 5$, $\lambda_4 = 7.1927$

Figure. 17 Fourth mode -3 types of Joint flexibility.

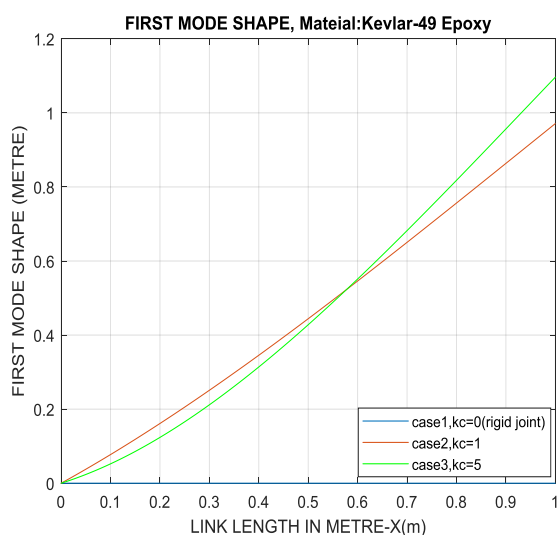
The first mode cases of vibration amplitude i.e., case-1 (stiffness co-efficient $k_c = 0$) is not equal to zero. Case-2 (stiffness co-efficient $k_c = 1$) is 0.39m, case-3 (stiffness co-efficient $k_c = 5$) is 0.89m. The second mode amplitude of case1, i.e. rigid mode stiffness co-efficient ($k_c = 0$) is 1.8980m, case-2 (stiffness co-efficient $k_c = 1$) is 1.8980m, case-3 (stiffness co-efficient $k_c = 5$) is 1.8980m and reduced. For third mode amplitude for case-1 ($k_c = 0$), case-2 ($k_c = 1$), and case-3 ($k_c = 5$) are same as third mode respectively. But the amplitude is decaying. From the fourth mode maximum amplitude vibration is reduced as shown in fig (17).

Table. IV Simulation Result Kevlar-49/Epoxy

| SL No. | Modes | Stiffness Coefficient Cases | Amplitude of Vibration (m) | Results obtained Compared to Other materials |
|--------|--------|-----------------------------|----------------------------|--|
| 1 | First | $k_c = 0$ | 0 | Zero value |
| 2 | | $k_c = 1$ | 0.39 | Low amplitude |
| 3 | | $k_c = 5$ | 0.89 | Low amplitude |
| 4 | Second | $k_c = 0$ | 1.898 | Low amplitude |
| 5 | | $k_c = 1$ | 1.898 | Low amplitude |
| 6 | | $k_c = 5$ | 1.898 | Low amplitude |
| 7 | Third | $k_c = 1,2,5$ | Less value | Neglected |
| 8 | Fourth | $k_c = 1,2,5$ | Less value | Neglected |

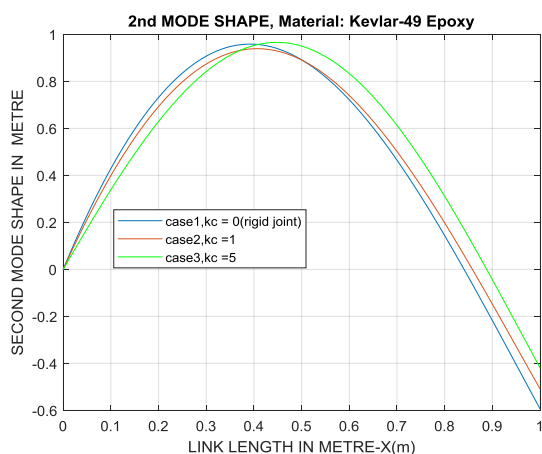
F. KEVLAR-49/ EPOXY MODE SHAPES 1, 2

Fig (14) to fig (17) gives the first mode shape links and node is reduced. The second mode shape for three flexible links at different position along the single link manipulator and up to $x = 1m$ and the node is shifted to the left of the link.



Case 1: $k_c = 0, \lambda_0 = 0$,
Case 2: $k_c = 1, \lambda_1 = 0.965716$,
Case 3: $k_c = 5, \lambda_1 = 1.100850$.

Figure 18 first mode shapes for three cases



Case 1: $k_c = 0, \lambda_1 = 2.630312$, Case 2: $k_c = 1, \lambda_2 = 2.789944$,
Case 3: $k_c = 5, \lambda_2 = 3.217521$.

Figure 19 second mode shapes for three cases

VI. CONCLUSION

In this article, equation of motion of single robotic link was derived. The state space model system was obtained. For numerical calculation purpose, three hybrid composite materials were taken for MATLAB simulation. The Eigen values (λ_i) were found from characteristic equation of flexible link system, the corresponding natural frequencies, modes and mode shape are evaluated. It was noticed that the values of third and fourth mode were numerically low and also observed that the amplitude of higher mode are quantitatively less, therefore the first two modes are calculated and recommended to use for control system design. The joint stiffness co-efficient was increased which cuts down the amplitude vibration and total deflection are noticed from the plots. The nodes in the mode shape were shifted towards to left side of the link and Kevlar-49 composite has given less amplitude of vibration (table-IV) among the three composite materials.

REFERENCES

- Malgaca, L., et.al, Effect of joint flexibility on vibration characteristics of a composite Box manipulator, Composite Structures, (2017)
- G. Venkata Narayanaa et.al, Modelling and control of single link manipulators for Flexible operation by using linearization techniques, International Journal of current Engineering and technology, Vol.3, No.2 (June 2013)
- Run-Min Hou, et.al, Hybrid Control Method for a Flexible Manipulator, IOP Conf. Series: Materials Science and Engineering 392, (2018), 062170, doi: 10.1088/1757-899X/392/6/062170
- B.S Reddy, A. Ghosal, Nonlinear dynamics of a rotating flexible link, Journal of Computational and nonlinear dynamics, vol, 10, no 6, (2015), 061014, pp.1-8
- Ramalingam S, Rasool Mohideen S, Hybrid Polymer Composite Flexible Multi-Link Robotic Manipulator Simulation Analysis, International Journal of Recent Technology and Engineering (IJRTE) ISSN: 2277-3878, Vol-7 Issue-6S2, April 2019
- Roy R, Craig, Structural dynamics, An Introduction to computer methods, (1981), pp.34- 35. John Wiley & sons' publication, 5th Edition, (2010), pp.159-225.
- H.N. Rahimia & M. Nazemizadeh, Dynamic analysis and intelligent control techniques for flexible manipulators: a review, Advanced Robotics, 2014, Vol.28, No.2, 63-76, <http://dx.doi.org/10.1080/01691864.2013.839079>.
- Guo-Ben Yang and Max Donath, Dynamic model of a one-link robot manipulator with both structural and joint flexibility, (1988), IEEE, pp.476-481.
- Ramalingam S, Rasool Mohideen S, Numerical Analysis of Robotic Manipulator Subject to Mechanical Flexibility by Lagrangian Method, Proc. National Academy of Science., India, Section. A Phys. Sci. <https://doi.org/10.1007/s40010-019-00619-2>.
- Ramalingam S., Roosal Mohideen S., Manigandan S. & T. P. Prem Anand, Hybrid Polymer composite material for robotic manipulator subject to single link with flexibility, International Journal of Ambient Energy, (2018), 1-8.
- Katsuhiko Ogata, Modern control engineering, PHI publication, 5th Edition, (2010), pp.159- 225.
- Asad A.K. M, Tokhi M.O, Modeling of a single link flexible manipulator system: Theoretical and practical investigations, Flexible Robot manipulators, published by IET, Control Series 68, (2008), pp. 23- 46.
- Jefferin Jose. P, Dynamics and control of flexible composite robotic manipulators based on finite element method, MTech, Project report, (2015), p.32.
- Ramalingam S, Rasool Mohideen S., Composite materials for advanced flexible link robotic manipulators: an investigation, International Journal of Ambient Energy, <https://doi.org/10.1080/01430750.2019.1613263>.
- Khalil Ibrahim A, et.al, Mode shape analysis of a flexible robot arm, International Journal of control automation and systems, (2013), vol.1, No. 2

AUTHORS PROFILE



Ramalingam S, Research scholar, B.E Graduate from Coimbatore Institute of Technology and M.E in Automation and Robotics from Osmania University, Hyderabad. At present, doing PhD in Robotics from B S A Cerescent Institute of Science and Technology, Chennai. He has published 6 papers in international journals and attended national and International seminars. He is member of IET, ISHMT, WWVA and Chartered Engineer (I). He worked as an Engineer for 15years in Industry and 10years for teaching in Engineering and Technology institutions. He is reviewer for few Internationals journals, His area of interest are Robotics, Design and analysis, Composite materials and Control systems.



Dr. Rasool Modideen S, Professor and Dean, School of Mechanical science, B S A Crescent Institute of Science and Technology, Chennai. He is supervisor for PhD students. He has published 32 papers in National and International Journals. Email Id: dean.sms@crescent.education



Prof. Sridhar P S, Marine Chief Engineer, He worked as a Marine Engineer for 30 years and at present working as a professor in Marine department in AMET university, Chennai. His area of interest is Ship construction, Marine Boilers, Marine auxiliary machines. He is supervisor for marine engineering students' projects. Email Id: monathatha @gmail.com